Title: Myelinating Schwann cells use Warburg effect to sustain axonal physiology and function

One Sentence Summary: Lactate-dependent axons rely on cancer-like metabolism in myelinating Schwann cells.

Authors: Marie Deck[1], Gerben Van Hameren[1], Graham Campbell[1], Nathalie Bernard-Marissal[2], Jérôme Devaux[1], Jade Berthelot[1], Alise Lattard[1], Jean-Jacques Médard[3], Benoît Gautier[1], Patrice Quintana[1], Juan Manuel Chao de la Barca[4,5], Pascal Reynier[4,5], Guy Lenaers[5], Roman Chrast[3], Nicolas Tricaud[1]*

Affiliations:

[1] INM, INSERM, Université de Montpellier, 80 Rue A. Fliche, 34090 Montpellier, France.

[2] Aix-Marseille Univ, INSERM, MMG, 13385 Marseille, France

[3] Departments of Clinical Neuroscience and Neuroscience, Karolinska Intitutet, Stockholm, Sweden.

[4] Département de Biochimie et Génétique, Centre Hospitalier Universitaire, Angers, France.

[5] Equipe Mitolab, MITOVASC, CNRS 6015, INSERM U1083, Université d'Angers, Angers, France.

*Correspondence to: nicolas.tricaud@inserm.fr (lead contact)

Summary: Whether glial cells use a particular metabolism to support axonal metabolism and function remains controversial. We show here that the deletion of PKM2, an enzyme essential for the Warburg effect, in mature myelinating Schwann cells (mSC) of mice leads to a deficit of lactate in these cells and in peripheral nerves, and to motor defects despite no alteration of the myelin sheath. When electrically stimulated, peripheral nerve axons of mutant mice failed to maintain lactate homeostasis, resulting in an impaired production of mitochondrial ATP. Action potential propagation was not changed but axonal mitochondria transport was altered, muscle axon terminals retracted and motor neurons showed cellular stress. Further reducing lactate availability through dichloroacetate treatment definitely aggravated axonal malfunction in mutant mice. Thus, cancer-like Warburg effect is essential in mSC for the long term maintenance of peripheral nerve axons physiology and function.

INTRODUCTION:

Energetic metabolism is an essential parameter of neurons' function and survival (Alle et al., 2009; Attwell and Laughlin, 2001; Harris and Attwell, 2012). Indeed, the nervous system consumes a large amount of glucose mainly to allow synapses to function but also organelles and vesicles transport along axons and action potentials firing (Harris and Attwell, 2012). In the peripheral nervous system (PNS), axons grow far from their cell bodies to reach distant targets such as muscles. Maintaining metabolic homeostasis on such a long distance is a real challenge for large axons that are extensively covered by a myelin sheath (Waxman, 1997).

This insulating sheath, resulting from several turns of compacted plasma membrane, is produced by myelinating Schwann cells (mSC). The ionic and electronic insulation forces action potentials to "jump" from one node of Ranvier to the next, accelerating the nerve conduction velocity up to

120m/s (Waxman, 1980). Unfortunately, this insulation also mechanically hinders the diffusion of metabolites in the axonal environment and prevents the metabolic supply of myelinated axons.

On the other hand, glial cells may be a solution to provide trophic support to the axons they surround. Evidence for a metabolic coupling between glial cells and neurons have been provided in the CNS. Indeed, astrocytes and oligodendrocytes play a critical role in this process by metabolizing glucose into lactate and exporting it to the axon as a fuel for axonal mitochondria, a process known as the lactate shuttle theory (Fünfschilling et al., 2012; Lee et al., 2012; Magistretti and Allaman, 2015). Recently, mitochondrial respiration was shown to be dispensable for myelinating oligodendrocytes suggesting these cells can use glycolysis for ATP production and produce lactate (Fünfschilling et al., 2012). Moreover, the disruption of monocarboxylate transporters (MCT), which mediate the traffic of metabolites in these cells, induces axonal damages and the degeneration of neurons *in vivo* (Lee et al., 2012), suggesting lactate export from oligodendrocytes is required for axons maintenance. In the PNS, mSC do not remain without mitochondrial respiration (Fünfschilling et al., 2012), but lactate has been detected in the extracellular space of nerves and shown to be effective in supporting nerve function *ex vivo* (Brown et al., 2012). So, the cellular origin of the released lactate and its relevance as an energy substrate for axons remains largely unclear.

Lactate production in aerobic conditions has been well studied in cancer cells. Indeed, many type of cancer cells use aerobic glycolysis, also called the Warburg effect, to produce ATP as well as other metabolites required for cell survival and proliferation (Vander Heiden et al., 2009). This metabolic shift to the Warburg effect relies on the expression of Pyruvate Kinase M2 (PKM2) isoform instead of PKM1 (Israelsen et al., 2013). PKM2 is a master regulator of glycolysis cumulating metabolic and non-metabolic functions as a protein kinase and transcriptional

coactivator (He et al., 2017). How PKM2 expression leads to more lactate is not clear. However, as PKM2 slows down pyruvate synthesis compared to PKM1, this may allow lactate dehydrogenase to metabolize pyruvate into lactate (Frezza and Gottlieb, 2009; Hanahan and Weinberg, 2011; He et al., 2017). Manipulating metabolism in cancer cells has emerged has an attractive avenue to treat tumors (Luengo et al., 2017). Dichloroacetate (DCA), a compound that indirectly activates pyruvate dehydrogenase (PDH) and increases the mitochondrial uptake of pyruvate, depletes cellular lactate and prevents cancer cells growth in several tumors (Stacpoole, 1989; Tataranni and Piccoli, 2019). DCA is also indicated to treat acute and chronic lactic acidosis and diabetes (James et al., 2017). However, a major side effect of DCA treatment is a reversible peripheral neuropathy from an unknown origin (James and Stacpoole, 2016; Tataranni and Piccoli, 2019).

We investigated the role of PKM2 and lactate homeostasis in mSC regarding the peripheral nerve axons physiology and function in mice. We found that PKM2 expression is upregulated during the maturation of mSC. Conditional deletion of PKM2 in myelinating cells during myelin maturation resulted in a deficit of lactate in mSC and in sciatic nerves of mutant mice. This resulted in a deficit of lactate in the cytoplasm of mutant mice axons when electrically stimulated. While cytoplasmic glucose level increased, mitochondria failed to upregulate their level of ATP in the matrix in these conditions. These cellular changes correlated with a deficit of performance in Rotarod and grip tests, indicating a peripheral neuropathy in mutant mice. However, both the myelin sheath and the nerve conduction velocity (NCV) were not altered, suggesting functional defects occurred in axons. Indeed, we found that neuromuscular junctions retracted in the gastrocnemius muscle and mitochondrial movements were slowed-down in peripheral nerves axons of mutant mice, showing that the peripheral neuropathy results from defects in axonal functions. Finally, while treatment

with DCA induced a reversible peripheral neuropathy in control mice, this neuropathy was found irreversible in mutant mice indicating that lactate production in mSC is critical to restore axonal functions following lactate depletion.

RESULTS:

PKM2 expression promotes Warburg effect in mature mSC

It is well accepted that PNS myelination starts at postnatal days 2-5 (P2-P5) in mice and, after an exponential phase, slows down by P30 to stop at 6 months postnatal (Cotter et al., 2010; Fernando et al., 2016). We therefore investigated the expression of PKM1 and PKM2 isoforms in mouse sciatic nerves at early and late stages of myelination. PKM1 mRNA was downregulated during sciatic nerve maturation from postnatal day (P) 2 to P28 while PKM2 expression increased at the same time (**Fig. 1A**). At early ages, P4 and P15, PKM1 and PKM2 were both expressed in mSC (E-cadherin) that surrounded axons (2H3, **Fig. 1B a,b,c,d**). At P30 and 5 months, PKM2 replaced PKM1 in mSC (**Fig. 1B e,f,g,h**), in particular in the perinuclear region (**Fig. S1**), suggesting mSC enters the Warburg effect metabolic mode when the myelinated fibers mature.

PKM2 deletion in mSC leads to a reorganization of the metabolism in the nerve

We then specifically and conditionally deleted PKM2 isoform in myelinating glia of mice crossing a mouse strain expressing floxed PKM2-specific exon 10 alleles (Israelsen et al., 2013) with a strain expressing the Cre recombinase under the inducible and myelinating cell-specific promoter PLP1-ERt (Doerflinger et al., 2003). Injecting tamoxifen in Cre positive/*PKM2*$^{fl/fl}$ (mutant) and Cre-negative/*PKM2*$^{fl/fl}$ (control) littermates at 1 month postnatal resulted in a significant decrease of PKM2 expression in sciatic nerves of mutant as seen in immunoblotting, quantitative RT-PCR and immunostaining (**Fig. 1C,D,E**). The same experiments indicated that

PKM1 was re-expressed in PKM2-deleted mSC (**Fig. 1D,E**), suggesting a compensatory mechanism to maintain glycolysis.

Next, we expressed a lactate-detecting fluorescent probe (Laconic, **Fig. S2,** San Martín et al., 2013) in mSC of the mouse sciatic nerve *in vivo* using an AAV9 vector (Gonzalez et al., 2014). Mutant and control mice expressing the probe were then anesthetized and their nerves imaged using a multi-photon microscope (Gonzalez et al., 2015) to measure the relative amount of lactate in mSC of living mice. Cells of mutant mice showed significantly less lactate than mSC of control mice (**Fig. 1F**). In addition, this deficit of lactate resulted in a reduced amount of lactate in mutant mice nerves compared to control ones (**Fig. 1G**).

A targeted metabolomic screen done on mutant and control mouse nerves showed a decrease of some acylcarnitines in mutant mice (**Fig. S3**), without modification of the acylcarnitine/carnitine ratio (0.2707 vs 0.2739 in control and mutant respectively, P=0.77 two – tailed Student T-test). These acylcarnitines are involved in the transport of fatty acids across mitochondrial membranes before their degradation in carnitine and acetyl-CoA (Indiveri et al., 2011). So the maintenance of the ratio coupled to the decrease of acylcarnitines indicated a higher turnover, suggesting an increase of the mitochondrial activity. Moreover, it has been reported that deletion of TFAM1, a gene essential to maintain mitochondrial DNA and therefore functional respiratory complexes, in mouse mSC induces mitochondrial dysfunction and a dramatic increase of acylcarnitines (Viader et al., 2013). Our data suggested the opposite effect in our mutant mice, i.e. the upregulation of mitochondrial activity.

Lactate homeostasis and ATP production are impaired in axons of PKM2-SCKO mice

According to the lactate shuttle theory this decrease of lactate should also result in a shortage of axonal lactate. We investigated this assumption by expressing Laconic in peripheral

axons using an intrathecal injection of AAV9 vector in young pups (**Fig. S4A**). After tamoxifen recombination we performed live-imaging of probe-labeled axons that cross the saphenous nerve in anesthetized mice (**Fig. S4A**) (Gonzalez et al., 2015). While in resting conditions no difference could be seen between genotypes (**Fig. S5A**), when nerves were challenged with electrical stimulations, axonal lactate increased shortly after the stimulation in control but dropped in mutant mice (**Fig. 2A**). So, in the long term, control mice axons were able to maintain their lactate homeostasis while mutant mice axons could not (**Fig. 2A**, red line).

Beside lactate, another way axons may feed their mitochondria is glucose-derived pyruvate. Thus, we used a glucose-specific probe (FLII12Pglu-700uδ6, **Fig. S4B**) (Takanaga et al., 2008) to investigate glucose level in axons in the same conditions. While in resting axons a similar amount of glucose was found in both genotypes (**Fig. S5B)**, upon electrical stimulations glucose increased in axons of mutant mice while it remained stable in control mice (**Fig. 2B**), suggesting that axons of mutant mice mobilized glucose instead of lactate upon stimulations. We finally investigated the production of ATP by axonal mitochondria *in vivo* using a mitochondria-targeted fluorescent probe detecting ATP (ATeam, **Fig. S4C**) (Tsuyama et al., 2013). Again no difference could be seen in resting conditions (**Fig. S5C)**. However, when axons were stimulated mutant mice mitochondria failed to increase ATP production while this production increased in control mice (**Fig. 2C**). Thus, in absence of the Warburg effect in mSC, lactate homeostasis and mitochondria ATP production are impaired in electrically active axons, despite the mobilization of glucose.

Behavior impairment and neuromuscular junction loss in PKM2-SCKO mice are not due to demyelination

The metabolic changes in mutant mice axons resulted in motor defects in mutant mice as a longitudinal analysis revealed a significant deficit in both Rotarod and grip tests after PKM2 deletion in mSC (**Fig. 3A,B**). However, nerve conduction velocity of sciatic nerves was not altered **(Fig. 3C**) suggesting that the myelin sheath was not affected. Indeed, electron microscopy analyses showed correctly myelinated axons and a regular g-ratio in mutant mice (**Fig. S6**). The conduction of action potentials along myelinated axons was also not altered as the electrophysiological properties of sciatic nerve axons *ex vivo* were maintained even at very high firing frequencies (**Fig. S7, Table S**). Motor neuron number did not change in the spinal cord (**Fig. 3D**) but they displayed a higher expression of cleaved Caspase 3 (**Fig. 3E and S8**), a marker of neuronal stress and axonal degeneration (Mukherjee and Williams, 2017). Indeed, tracking axonal mitochondria *in vivo* revealed a decrease of their movements in mutant mice both before and after electrical stimulation (**Fig. 3F**). In addition, mutant mice showed significantly more denervated neuromuscular junctions with intact postsynaptic structures (**Fig. 3G,H**) in the gastrocnemius muscle, suggesting the retraction of axon terminals. Taken together, these data indicated that the Warburg effect in mSC is required for the maintenance of axonal trafficking and neuromuscular junctions.

Long-term maintenance of axons function rely on lactate feeding by SC

To investigate this further, we treated mutant and control mice with dichloroacetate (DCA), a drug that promotes mitochondrial consumption of pyruvate and decreases the availability of lactate (**Fig. 4A**)(Stacpoole, 1989). As previously observed in rodents and some patients (James and Stacpoole, 2016), this treatment induced an axonal peripheral neuropathy in mice: their Rotarod performance decreased independently of the genotype (**Fig. 4B**) while the nerve conduction velocity did not significantly change (**Fig. 4C**). When the treatment stopped control

mice totally recovered after 3 weeks while mutant mice did not (**Fig. 4B**). This indicated that axonal function was definitely damaged in these mice, confirming that Warburg effect in mSC is required for the long-term maintenance of peripheral axons' physiology.

DISCUSSION:

While the role of the lactate in the metabolic crosstalk between axons and the surrounding glia has been recognized for a long time in the CNS (Harris and Attwell, 2012), it remains unclear in the PNS. The presence of this compound in peripheral nerves had been detected and *ex vivo* experiments had shown that it could support action potentials propagation along axons (Brown et al., 2012). However, the origin of this nerve lactate remained unclear. Deleting PKM2 in mSC *in vivo* showed that part of this nerve lactate is provided by mSC using aerobic glycolysis and this lactate is required for axons to maintain their metabolic homeostasis and functions over time.

Unexpectedly, and to the opposite of cancer cells, preventing mSC performing aerobic glycolysis had very little impact on its own physiology and biology. Indeed, no defect could be detected in the myelin sheath of PKM2 mutant mice and the nerve conduction was not affected. A slight but significant shift occurred in the amount of some acylcarnitines without any alteration of the carnitine/acylcarnitine ratio, suggesting a higher turnover of these compounds that shuttle lipids into mitochondria for β-oxidation. According to the literature we interpreted these data as the sign of a higher metabolic activity of mSC mitochondria (in the nerve most of the mitochondria are in mSC). This is consistent with the upregulation of PKM1 expression we observed in mutant mice nerves as the higher enzymatic activity of this isoform promotes pyruvate production and its use in the mitochondrial Krebs cycle and respiration. So, in the absence of PKM2, mSC metabolism probably shifted to more oxidative phosphorylation. As mSC cannot be dispensed of

mitochondrial respiration (Fünfschilling et al., 2012), this shift is likely to be mild for the cell which is still able to produce myelin and maintain it. However, the shutdown of aerobic glycolysis in mSC is clearly deleterious for axonal maintenance showing mSC actively uses this metabolic mode in wild type conditions. So, we conclude that mSC use simultaneously both mitochondrial respiration for myelin production and maintenance and Warburg effect to support axons survival.

The challenge in the analysis of metabolic crosstalk in a tissue is to distinguish between the metabolisms of the different cell types. In addition, nerve injury or section immediately modifies both axonal (Kerschensteiner et al., 2005) and glial (Gonzalez et al., 2015) mitochondria physiology. To overcome these challenges, we chose to use the genetically encoded fluorescent probes delivered specifically to axons or mSC *in vivo* to follow a few critical metabolites in real time in physiological conditions. These probes such as lactate sensor *Laconic*, the glucose sensor *FLII12Pglu-700u&6* and the ATP sensor *ATeam* have been extensively characterized in several *in vitro* and *in vivo* models and we confirmed that variations could be observed in the nerve *in vivo*. Of course this gave us a limited view of all the metabolic changes that may have occurred in mutant cells, but we could nevertheless draw some decisive conclusions.

Firstly, we observed that the metabolic homeostasis is really efficient in peripheral nerves. While electrically activated axons show radical alterations in mutant mice in just a few dozens of minutes in particular for lactate, no change could be detected in resting axons of anesthetized animals disregarding the genotype. So, in just 20 minutes, the time it takes to anesthetize a mouse, expose the nerve under the microscope and image, metabolic homeostasis is able to bring all the metabolites we analyzed to their resting values. In this regard, axonal homeostasis is much more efficient than mSC homeostasis as lactate levels remained significantly lower in these cells in mutant mice than in control mice. However, axonal homeostasis was not sufficient to buffer the

metabolic changes that occur following physiological stimulations. Indeed, while axonal lactate remained apparently unaltered after stimulations in control mice, it sharply and steadily dropped in mutant mice axons. This revealed that actually the maintenance of lactate levels in control mice axons is due to a significant uptake of mSC lactate to compensate for a severe consumption during axonal activity. So, lactate produced by mSC is a critical fuel for mitochondria of actively-firing myelinated axons. Indeed, even the mobilization of glucose in stimulated axons was not sufficient to sustain an adequate ATP production in mitochondria. The involvement of the mSC lactate was definitively confirmed by the DCA treatment. Mutant mice were unable to recover their performances on the Rotarod following the draining of lactate supplies, while mice that could produce lactate in their mSC through aerobic glycolysis recovered. This underlines the addiction of myelinated axons to mSC lactate as all the other sources of energy substrates such as glucose, glycogen or glutamine are not directly altered by DCA. The reason for this addiction is puzzling but one possibility could be the swift accessibility of this glial lactate pool and its readiness for mitochondrial respiration while using glucose may require more time and enzymatic resources in the axons to generate pyruvate.

The main macroscopic phenotype resulting from PKM2 deletion in mSC is a motor weakness observed through Rotarod and grip test in the absence of demyelination. This was not significantly detectable before 6 months suggesting a late onset of the neuropathy. Taken together this is characteristic of axonal CMT diseases in mice. Moreover, this neuropathy did not result from motor neurons death but from an axonal dysfunction illustrated by a decreased mitochondrial motility and retracted neuromuscular terminals. This retraction is likely to be the main cause of the motor weakness. Mitochondrial migration, which is essential for the maintenance of the synapses, in particular in motor neurons (Marinković et al., 2012), relies on the ATP produced in

mitochondria. In a previous work we showed that shutting down ATP synthase activity steadily slowed down mitochondrial movements in mSC *in vivo* (Gonzalez et al., 2015). So, the failure of mutant mice axonal mitochondria to increase their ATP production following physiological activity is likely to the initial cause of the axonal dysfunction.

However, axonal firing properties were not significantly altered by this mitochondrial failure. This was unexpected because a largely accepted idea is that axonal ATP, and therefore axonal mitochondria, are required to maintain the membrane negative potential that allows depolarization. Actually, more recent analysis of neuronal energetics indicates that the energy cost of maintaining axon membrane potential is not that important, especially in myelinated fibers (Harris and Attwell, 2012). Therefore, the production of ATP by mutant mice axonal mitochondria may be sufficient to support this cost. Alternatively, the ATP required for the function of Na/K ATPase may not be provided by mitochondria in axons. Indeed, the local production of ATP through glycolysis may be sufficient. A more thorough analysis of energetics in the node of Ranvier is required to answer this question. In any cases, our data clearly indicate that mitochondrial ATP production and adaptation to the axon activity is critical for axonal maintenance.

Meeting the energy demand of axons is critical to ensure the long term maintenance of the nervous system. Indeed, increasing evidences indicate that an unbalanced energy supply to axons is a capital factor of neurodegenerative diseases such as ALS (Vandoorne et al., 2018), Parkinson and Alzheimer diseases (Camandola and Mattson, 2017). However, the molecular basis of this support remains unclear. The present data show that axonal dysfunction may be a direct result of perturbed metabolic support by supporting glial cells such as mSC. In this regard, the dramatic effect of DCA treatment on control and mutant mice motor performances is striking and the

inability of mutant mice to recover from this treatment is challenging. Indeed, DCA is proposed as a long-term treatment for several cancers and other diseases such as acute and chronic lactic acidosis and diabetes. Our data suggest that drugs targeting aerobic glycolysis metabolism as a treatment for these diseases may have a singular and deleterious effect on the nervous system and in particular on the PNS. Therefore, further and finer characterization of the axon/glia metabolic crosstalk is required in particular in neurodegenerative diseases. In this regard, the cancer-like nature of this glial metabolism constitute a risk for the nervous system regarding the deleterious effects of anticancer drugs that affect cell metabolism.

Acknowledgments:

We thanks H.Boukhaddaoui, C.Sar, V.Baecker and the imaging facility MRI, the INM animal facility, L.Diouloufet and C. Cazevieille. European Research Council grant (FP7-IDEAS-ERC #311610), INSERM AVENIR, EpiGenMed Labex, The Neuromuscular Research Association Basel, Swedish StratNeuro program, Swedish Research Council grant (#2015-02394), and AFM-Téléthon (#20044).

Author contributions: Conceptualization: NT; Formal analysis: MD, GvH, JJM, JMCB; Funding acquisition: RC, NT; Investigation: MD, GvH, NBM, JD, GC, JB, AL, JJM, BG; Methodology: PQ; Project administration: PR, GL, RC, NT; Supervision: NT; Validation: MD, GvH, PR; Visualization: MD, GvH, JJM, NT; Writing – original draft: MD, GvH, NT; Writing – review & editing: all co-authors.

Competing interests: Authors declare no competing interests.

Figure Legends:

FIGURE 1 PKM2 is efficiently deleted in mature mSC of Mutant mice.

A- Quantitative RT-PCR on sciatic nerve extracts shows decreased PKM1 and increased PKM2 expressions during mSC maturation. Normalized on P2 values. n=4 animals.

B- Immunostaining on mouse sciatic nerve sections shows decreased PKM1 (left panels) and increased PKM2 (right panels) expressions in mSC. m: months. Sc:Schwann cell; a: axon.

C- Western blots on sciatic nerve extracts show lower PKM2 and higher PKM1 amounts in Mutant versus Control mice sciatic nerves (2 months old). Actin serves as loading control. n=3 mice.

D- Quantitative RT-PCR on sciatic nerve extracts shows decreased PKM2 and increased PKM1 expressions in Mutant (Mut, n=7) versus Control (Cont, n=5) mouse sciatic nerves (3 and 12 months old).

E- Immunostainings on sciatic nerve sections show PKM2 lower in Mutant mSC (panel l) while PKM1 is higher (arrowheads and Insert panel k)(2 months old).

F- The ratio of Laconic probe was measured in mSC of Mutant (n=11 mice, 41 cells) and Control (n=11 mice, 45 cells) anesthetized mice and normalized to the mean of Control values (7 to 10 weeks old mice).

G-Biochemical measure of lactate shows a reduced concentration in Mutant versus Control sciatic nerves (n=6 mice)(4 and 12 months old).

All scale bars = 10µm. Two-tailed Student t-test. Error bars represent SD (A, D) or SEM (F). AU: arbitrary unit.

FIGURE 2 Mutant mice axons display an altered metabolic response to electrical stimulations.

The ratio of fluorescent probes (R) was normalized over the average ratio at time points before the first stimulation (R0)(basal value). Segments at the top of each Control mice graphs show stimulation periods. Lines show the basal value line. Statistical analysis shows the test for linear trend following one-way ANOVA analysis. Error bars represent SEM.

A- n= 20 axons, 7 mice for Control and 7 axons, 4 mice for Mutant.

B- n= 6 axons, 3 mice for Control and 9 axons, 3 mice for Mutant.

C- n= 16 axons, 5 mice for Control and 14 axons, 5 mice for Mutant.

FIGURE 3 Mutant mice show motor deficit and display axonal defects.

A- Rotarod latency to fall and **B-** grip strength were measured between 2 and 16 months postnatal on Control (n=21) and Mutant (n=25) mice. Two-way non repeated measures ANOVA Sidak's post-hoc tests.

C- Nerve conduction velocity (NCV) measured in Control and Mutant mice (n=10 each). Two-way non repeated measures ANOVA Sidak's post-hoc tests.

D- Spinal cord sections of Mutant (Mut) and Control (Cont) mice (12 months) were stained with cresyl violet and motor neurons were counted (see Fig. S8). n= 3 animals (14 to 30 sections). Two tailed Student t-test.

E- Spinal cord sections of Mutant (Mut, n=19 images, 3 animals) and Control (Cont, n= 12 images, 2 animals) mice were immunostained for Caspase 3, ChAT and Neurofilament (Fig. S8) (12 months old). Caspase 3 positive neurons in percentage of Neurofilament positive neurons. Two tailed Student t-test.

F- Axonal mitochondria labelled with mito-Dsred2 were imaged *in vivo* before and after electrical stimulation. **Upper panels** show typical kymographs. Tracked mitochondria are shown with colour dots. Mutant mice mitochondria follow a straight pattern indicating they are immobile or slowly moving. **Lower panel**: Mitochondria speed was plotted according to the genotype before and after stimulation. One-way ANOVA Tukey's post-hoc test. n are provided in Material and Methods.

G- Gastrocnemius muscle neuromuscular junctions of 12 months old Mutant and Control mice were stained for presynaptic SV2 and postsynaptic acetylcholine receptor with FITC-α-bungarotoxin (α-bung). Scale bar= 100μm.

H- Innervated (inn, complete overlap), partially innervated (part, partial overlap) and denervated (den, no overlap) junctions were counted on sections as shown in D. Two tailed Student t-test. n= 4 mice (12 months).

Error bars represent SEM.

FIGURE 4 PKM2 deletion in mSC impairs motor performance recovery after DCA treatment.

A- Metabolic pathways directly affected by the manipulations. LDH: lactate dehydrogenase; PDH: pyruvate dehydrogenase; PDK: PDH kinase.

B- Rotarod latency to fall was measured in 9 months old Control (n=5) and Mutant mice (n=5) during a 7 weeks daily treatment with DCA and then during a three weeks recovery period without treatment. Two-way non repeated measures ANOVA Sidak's post-hoc test from week 7 to week 10.

C- Nerve conduction velocity (NCV) measured in 9 months old Control (n=5) and Mutant mice (n=7) at 0, 3 and 7 weeks of DCA treatment and 3 weeks after stopping the treatment (week 10). Two-way non repeated measures ANOVA statistical tests, Sidak's post-hoc tests over the 4 time points.

Error bars represent SEM.

List of Supplementary Materials:

Materials and Methods

Fig S1 – S8

Table S

References:

Alle, H., Roth, A., and Geiger, J.R.P. (2009). Energy-Efficient Action Potentials in Hippocampal Mossy Fibers. Science *325*, 1405–1408.

Attwell, D., and Laughlin, S.B. (2001). An Energy Budget for Signaling in the Grey Matter of the Brain. J Cereb Blood Flow Metab *21*, 1133–1145.

Brown, A.M., Evans, R.D., Black, J., and Ransom, B.R. (2012). Schwann Cell Glycogen Selectively Supports Myelinated Axon Function. Ann Neurol *72*, 406–418.

Camandola, S., and Mattson, M.P. (2017). Brain metabolism in health, aging, and neurodegeneration. EMBO J *36*, 1474–1492.

Cotter, L., Ozçelik, M., Jacob, C., Pereira, J.A., Locher, V., Baumann, R., Relvas, J.B., Suter, U., and Tricaud, N. (2010). Dlg1-PTEN interaction regulates myelin thickness to prevent damaging peripheral nerve overmyelination. Science *328*, 1415–1418.

Doerflinger, N.H., Macklin, W.B., and Popko, B. (2003). Inducible site-specific recombination in myelinating cells. Genesis *35*, 63–72.

Fernando, R.N., Cotter, L., Perrin-Tricaud, C., Berthelot, J., Bartolami, S., Pereira, J.A., Gonzalez, S., Suter, U., and Tricaud, N. (2016). Optimal myelin elongation relies on YAP activation by axonal growth and inhibition by Crb3/Hippo pathway. Nat Commun *7*, 12186.

Frezza, C., and Gottlieb, E. (2009). Mitochondria in cancer: Not just innocent bystanders. Seminars in Cancer Biology *19*, 4–11.

Fünfschilling, U., Supplie, L.M., Mahad, D., Boretius, S., Saab, A.S., Edgar, J., Brinkmann, B.G., Kassmann, C.M., Tzvetanova, I.D., Möbius, W., et al. (2012). Glycolytic oligodendrocytes maintain myelin and long-term axonal integrity. Nature *485*, 517–521.

Gonzalez, S., Fernando, R.N., Perrin-Tricaud, C., and Tricaud, N. (2014). In vivo introduction of transgenes into mouse sciatic nerve cells in situ using viral vectors. Nature Protocols *9*, 1160–1169.

Gonzalez, S., Fernando, R., Berthelot, J., Perrin-Tricaud, C., Sarzi, E., Chrast, R., Lenaers, G., and Tricaud, N. (2015). In vivo time-lapse imaging of mitochondria in healthy and diseased peripheral myelin sheath. Mitochondrion *23*, 32–41.

Hanahan, D., and Weinberg, R.A. (2011). Hallmarks of Cancer: The Next Generation. Cell *144*, 646–674.

Harris, J.J., and Attwell, D. (2012). The energetics of central nervous system white matter. J Neurosci *32*, 356–371.

He, X., Du, S., Lei, T., Li, X., Liu, Y., Wang, H., Tong, R., and Wang, Y. (2017). PKM2 in carcinogenesis and oncotherapy. Oncotarget *8*, 110656–110670.

Indiveri, C., Iacobazzi, V., Tonazzi, A., Giangregorio, N., Infantino, V., Convertini, P., Console, L., and Palmieri, F. (2011). The mitochondrial carnitine/acylcarnitine carrier: Function, structure and physiopathology. Molecular Aspects of Medicine *32*, 223–233.

Israelsen, W.J., Dayton, T.L., Davidson, S.M., Fiske, B.P., Hosios, A.M., Bellinger, G., Li, J., Yu, Y., Sasaki, M., Horner, J.W., et al. (2013). PKM2 isoform-specific deletion reveals a differential requirement for pyruvate kinase in tumor cells. Cell *155*, 397–409.

James, M.O., and Stacpoole, P.W. (2016). Pharmacogenetic considerations with dichloroacetate dosing. Pharmacogenomics *17*, 743–753.

James, M.O., Jahn, S.C., Zhong, G., Smeltz, M.G., Hu, Z., and Stacpoole, P.W. (2017). Therapeutic applications of dichloroacetate and the role of glutathione transferase zeta-1. Pharmacology & Therapeutics *170*, 166–180.

Kerschensteiner, M., Schwab, M.E., Lichtman, J.W., and Misgeld, T. (2005). In vivo imaging of axonal degeneration and regeneration in the injured spinal cord. Nat. Med. *11*, 572–577.

Lee, Y., Morrison, B.M., Li, Y., Lengacher, S., Farah, M.H., Hoffman, P.N., Liu, Y., Tsingalia, A., Jin, L., Zhang, P.-W., et al. (2012). Oligodendroglia metabolically support axons and contribute to neurodegeneration. Nature *487*, 443–448.

Luengo, A., Gui, D.Y., and Vander Heiden, M.G. (2017). Targeting Metabolism for Cancer Therapy. Cell Chemical Biology *24*, 1161–1180.

Magistretti, P.J., and Allaman, I. (2015). A Cellular Perspective on Brain Energy Metabolism and Functional Imaging. Neuron *86*, 883–901.

Marinković, P., Reuter, M.S., Brill, M.S., Godinho, L., Kerschensteiner, M., and Misgeld, T. (2012). Axonal transport deficits and degeneration can evolve independently in mouse models of amyotrophic lateral sclerosis. Proc Natl Acad Sci U S A *109*, 4296–4301.

Mukherjee, A., and Williams, D.W. (2017). More alive than dead: non-apoptotic roles for caspases in neuronal development, plasticity and disease. Cell Death Differ *24*, 1411–1421.

San Martín, A., Ceballo, S., Ruminot, I., Lerchundi, R., Frommer, W.B., and Barros, L.F. (2013). A genetically encoded FRET lactate sensor and its use to detect the Warburg effect in single cancer cells. PLoS ONE *8*, e57712.

Stacpoole, P.W. (1989). The pharmacology of dichloroacetate. Metabolism *38*, 1124–1144.

Takanaga, H., Chaudhuri, B., and Frommer, W.B. (2008). GLUT1 and GLUT9 as major contributors to glucose influx in HepG2 cells identified by a high sensitivity intramolecular FRET glucose sensor. Biochim. Biophys. Acta *1778*, 1091–1099.

Tataranni, T., and Piccoli, C. (2019). Dichloroacetate (DCA) and Cancer: An Overview towards Clinical Applications.

Tsuyama, T., Kishikawa, J., Han, Y.-W., Harada, Y., Tsubouchi, A., Noji, H., Kakizuka, A., Yokoyama, K., Uemura, T., and Imamura, H. (2013). In vivo fluorescent adenosine 5'-triphosphate (ATP) imaging of Drosophila melanogaster and Caenorhabditis elegans by using a genetically encoded fluorescent ATP biosensor optimized for low temperatures. Anal. Chem. *85*, 7889–7896.

Vander Heiden, M.G., Cantley, L.C., and Thompson, C.B. (2009). Understanding the Warburg effect: the metabolic requirements of cell proliferation. Science *324*, 1029–1033.

Vandoorne, T., De Bock, K., and Van Den Bosch, L. (2018). Energy metabolism in ALS: an underappreciated opportunity? Acta Neuropathol *135*, 489–509.

Viader, A., Sasaki, Y., Kim, S., Strickland, A., Workman, C.S., Yang, K., Gross, R.W., and Milbrandt, J. (2013). Aberrant Schwann cell lipid metabolism linked to mitochondrial deficits leads to axon degeneration and neuropathy. Neuron *77*, 886–898.

Waxman, S.G. (1980). Determinants of conduction velocity in myelinated nerve fibers. Muscle Nerve *3*, 141–150.

Waxman, S.G. (1997). Axon-glia interactions: building a smart nerve fiber. Curr. Biol. *7*, R406-410.

FIGURE 1

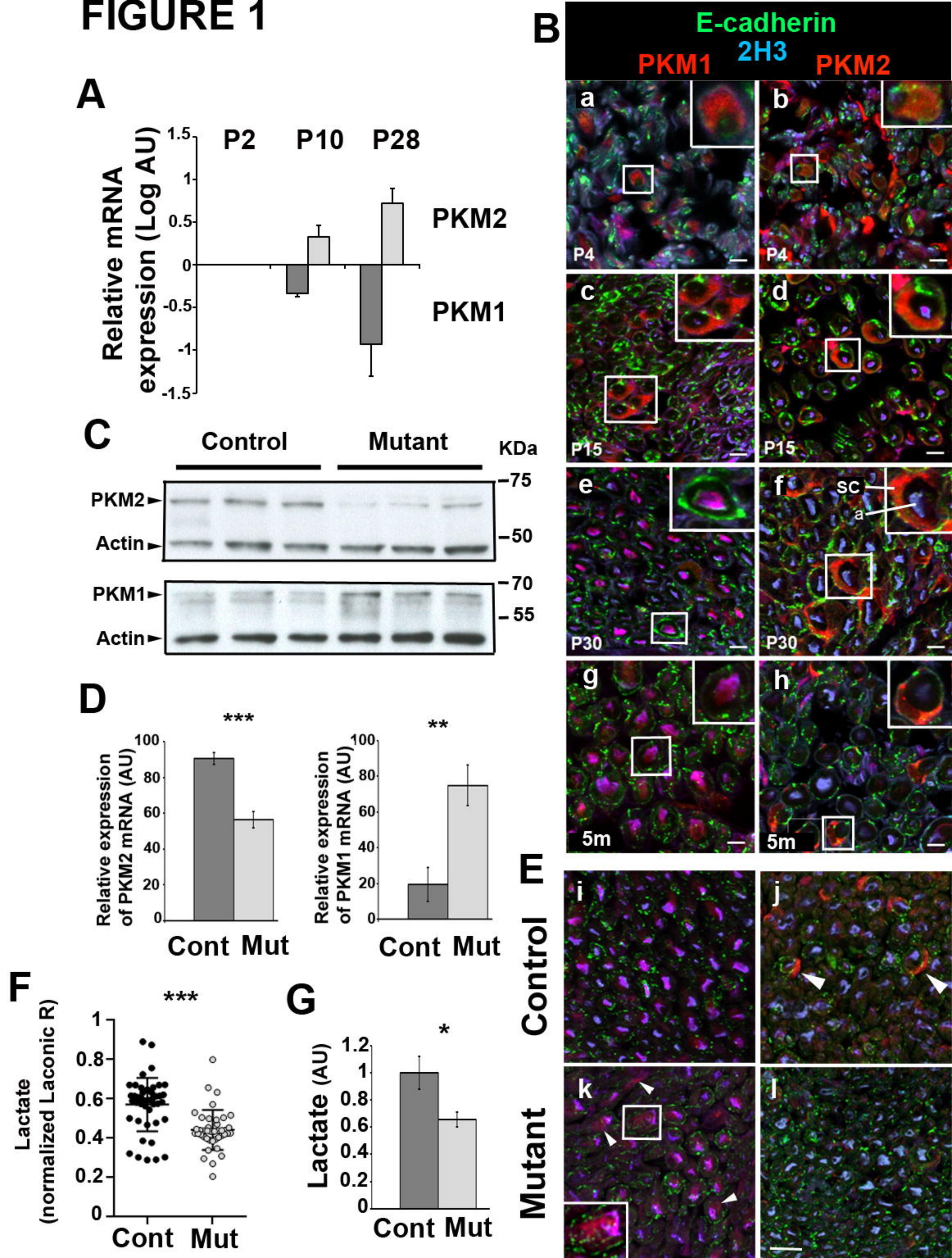
A
Relative mRNA expression (Log AU)
P2
P10
P28
PKM2
PKM1
B
E-cadherin
2H3
PKM1
PKM2
P4
P15
P30
5m
SC
a
C
Control
Mutant
KDa
PKM2
Actin
PKM1
Actin
75
50
70
55
D
Relative expression of PKM2 mRNA (AU)
Relative expression of PKM1 mRNA (AU)
Cont
Mut
E
Control
Mutant
F
Lactate (normalized Laconic R)
G
Lactate (AU)

FIGURE 2

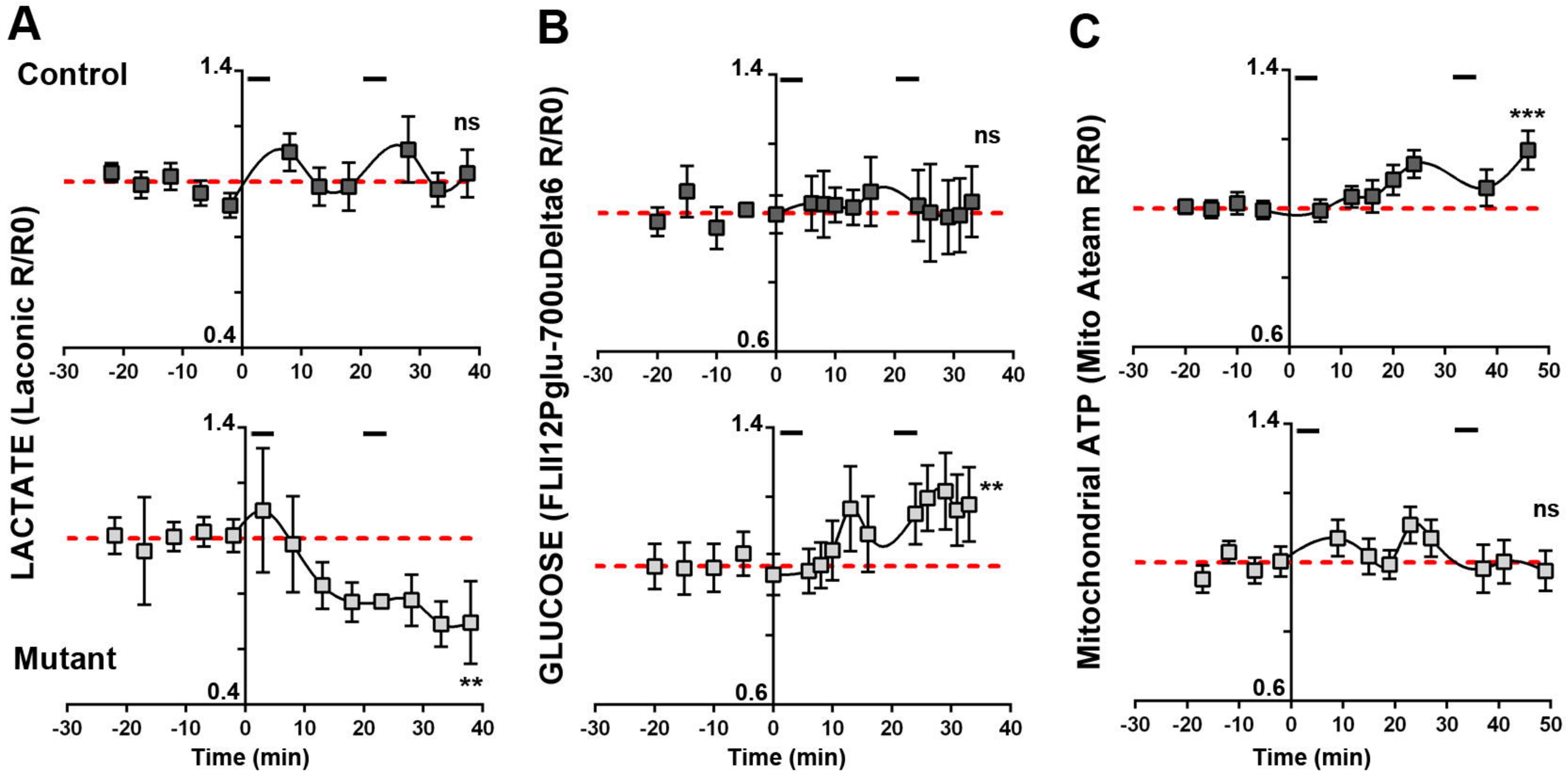
A
B
C
Control
Mutant
LACTATE (Laconic R/R0)
GLUCOSE (FLII12Pglu-700uDelta6 R/R0)
Mitochondrial ATP (Mito Ateam R/R0)
1.4
0.4
0.6
ns
**
***
-30
-20
-10
0
10
20
30
40
50
Time (min)

FIGURE 3

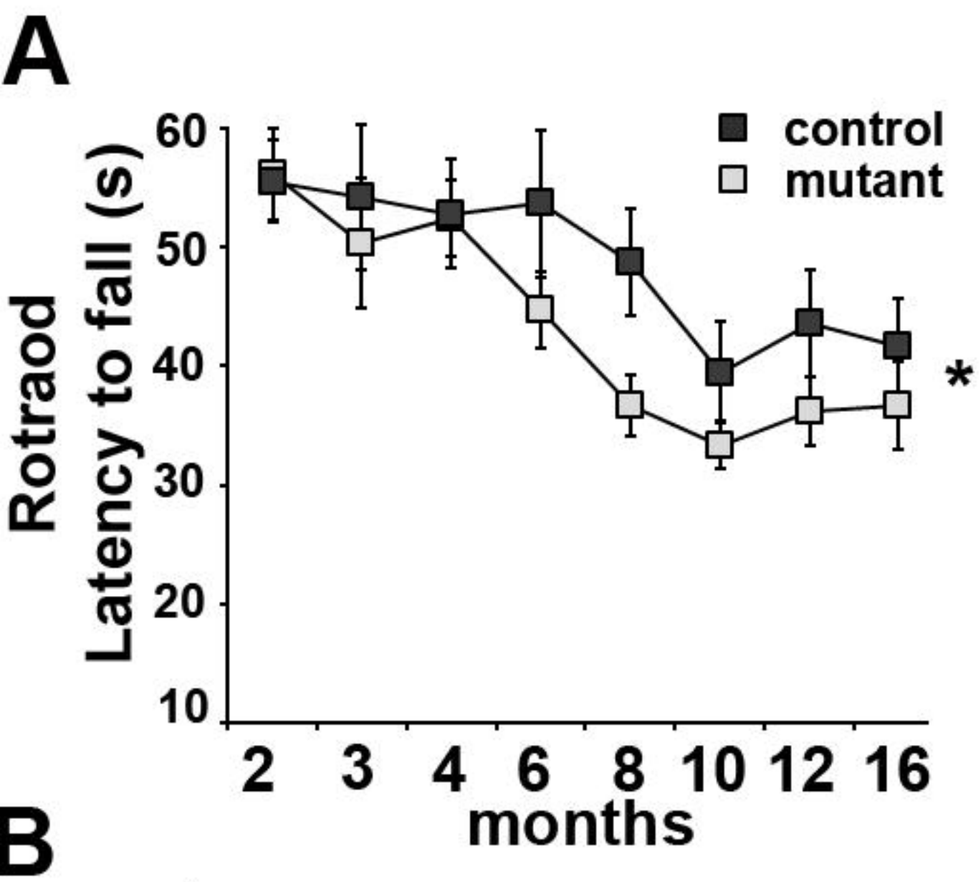
A
Rotraod
Latency to fall (s)
control
mutant
*
months

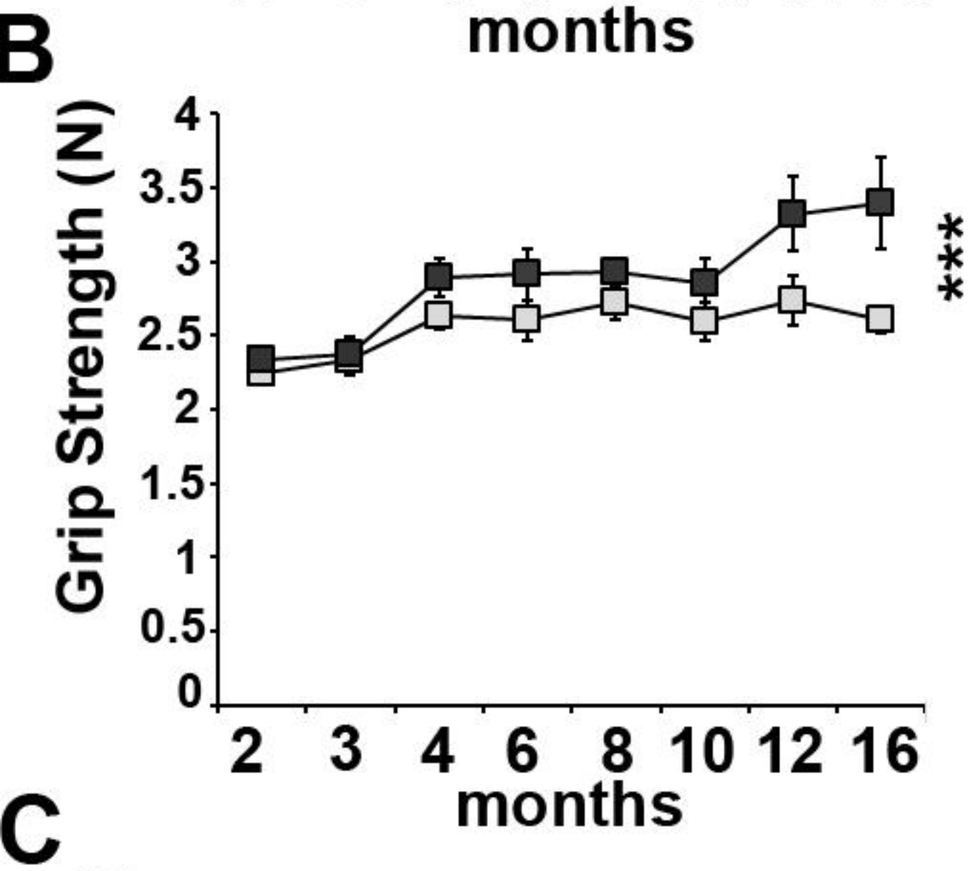
B
Grip Strength (N)
***
months

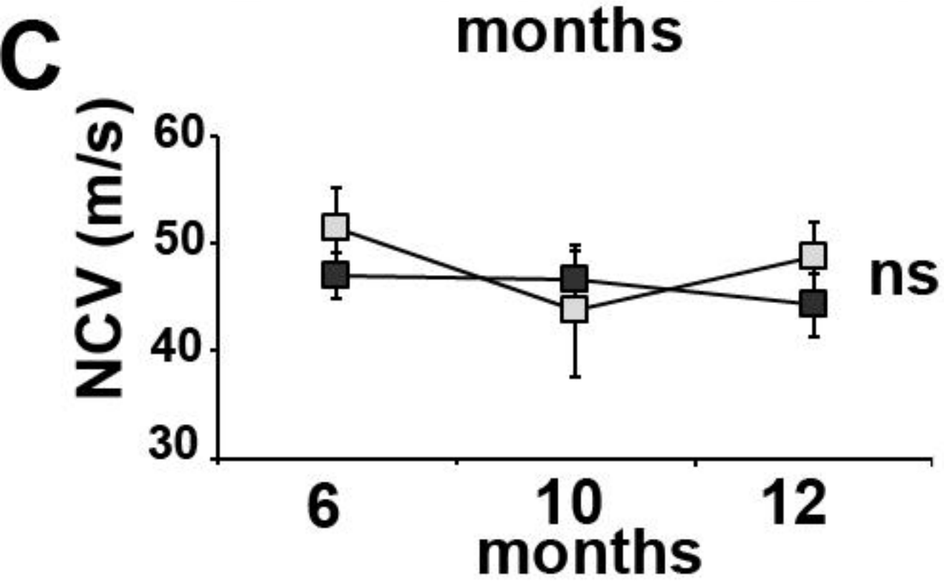
C
NCV (m/s)
ns
months

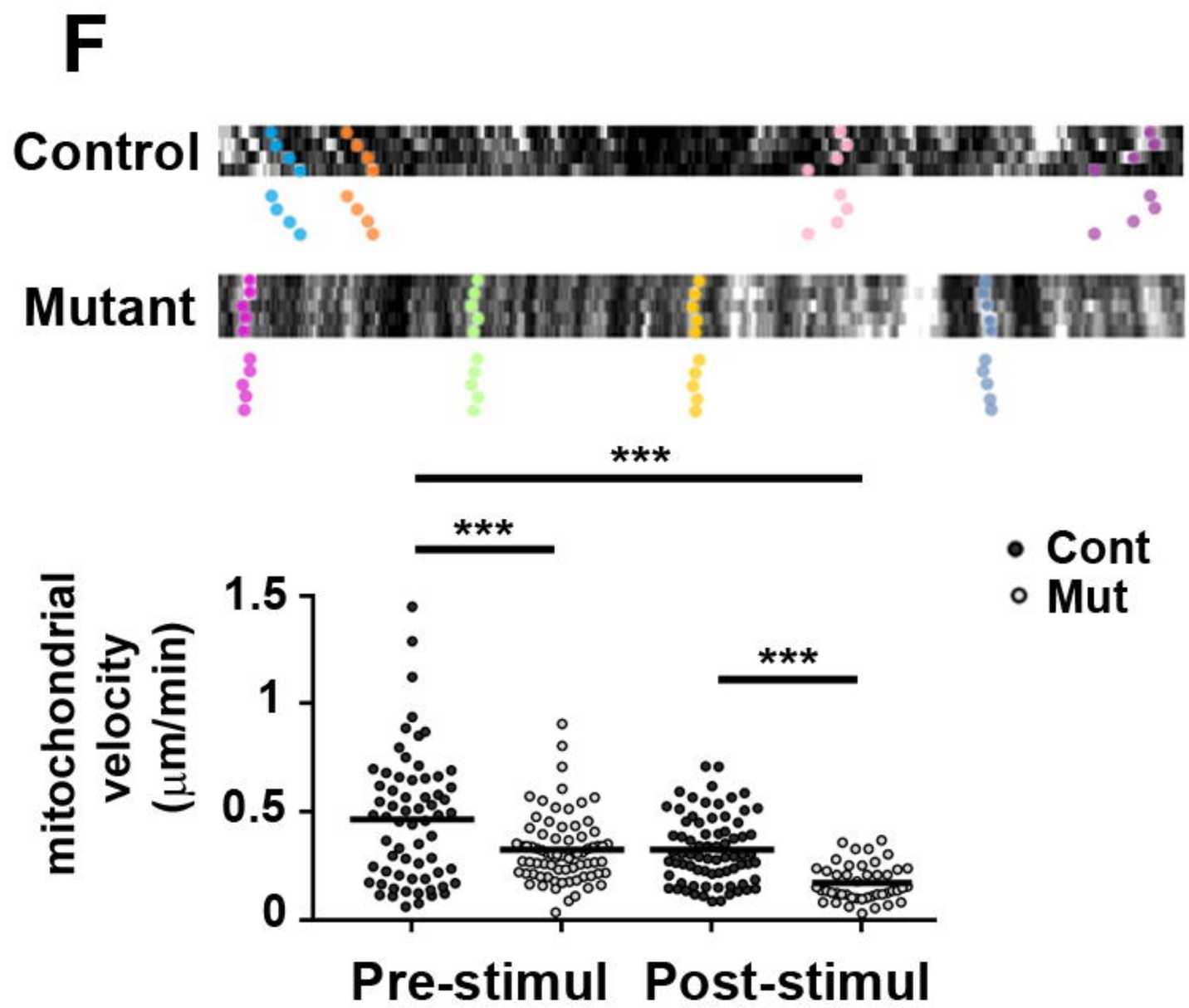
F
Control
Mutant
***
***
***
Cont
Mut
mitochondrial velocity (μm/min)
Pre-stimul
Post-stimul

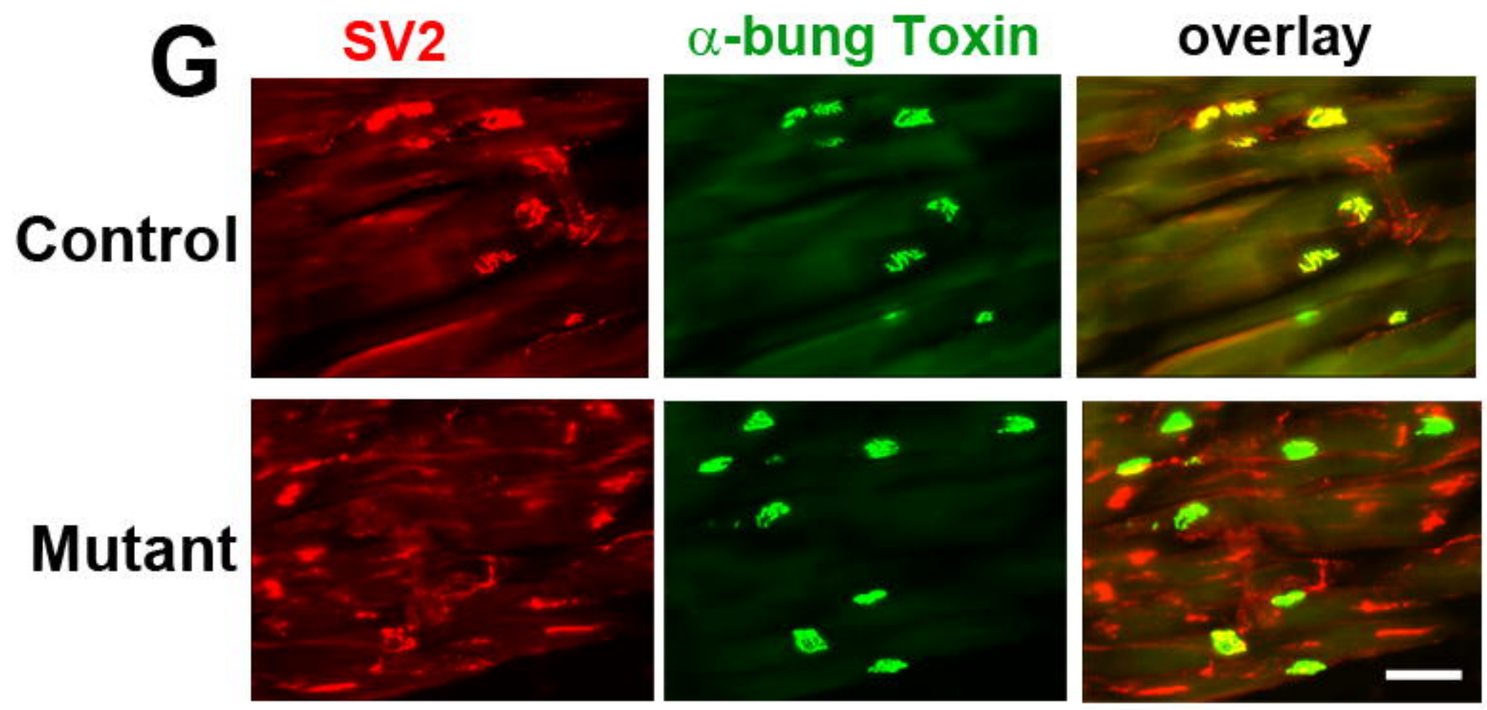
G
SV2
α-bung Toxin
overlay
Control
Mutant

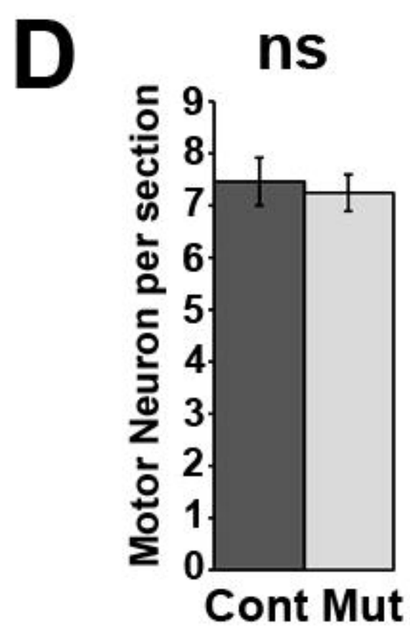
D
ns
Motor Neuron per section
Cont
Mut

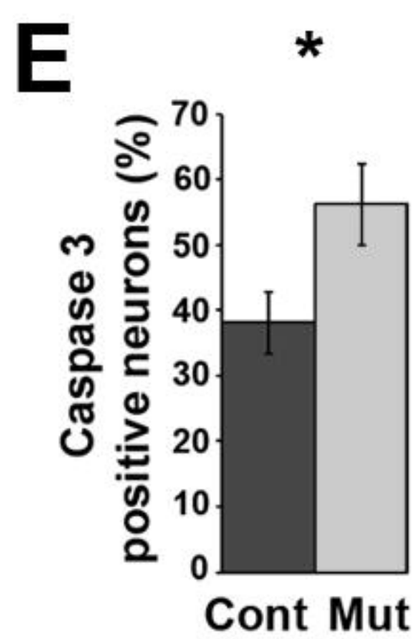
E
*
Caspase 3 positive neurons (%)
Cont
Mut

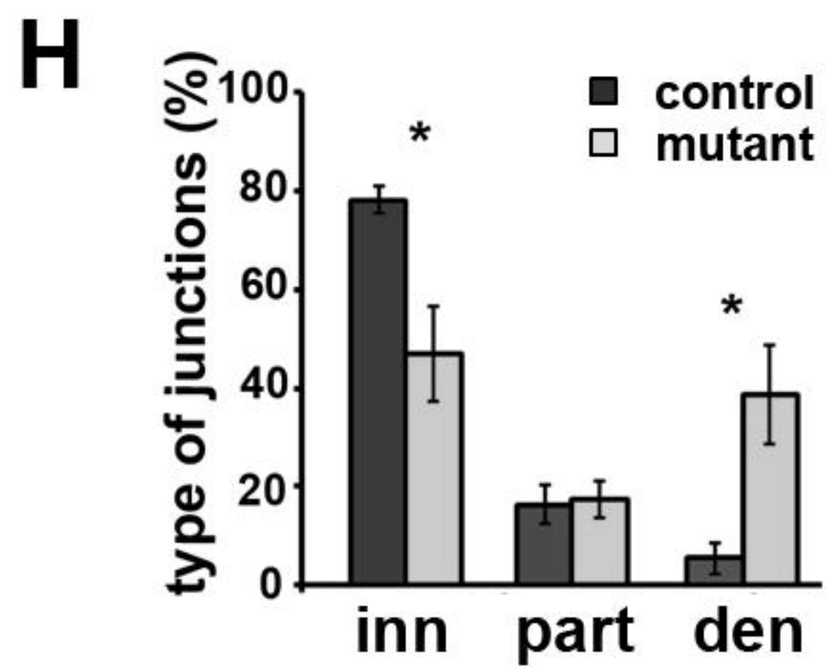
H
control
mutant
type of junctions (%)
*
*
inn
part
den

FIGURE 4

A

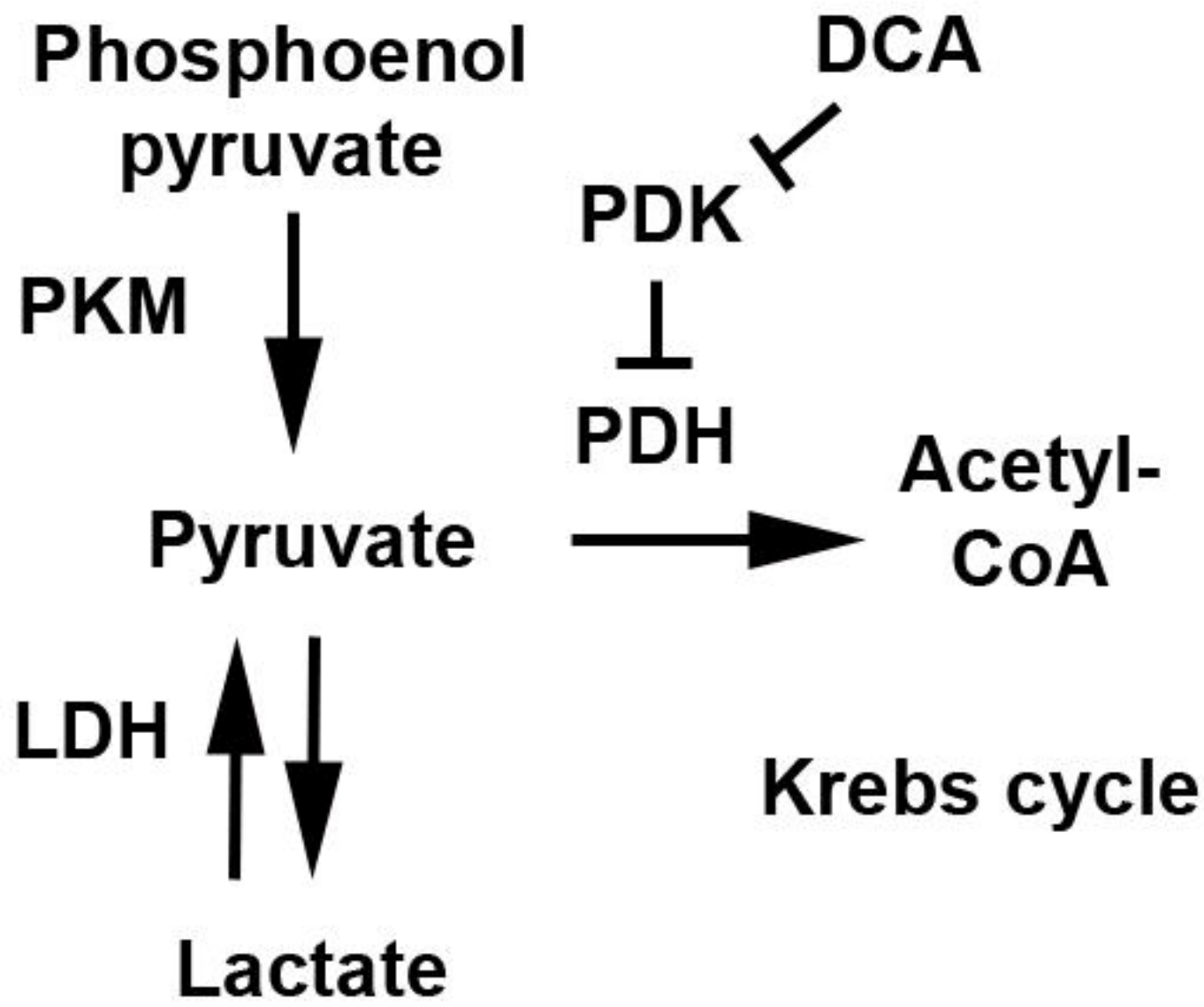
Phosphoenol pyruvate
DCA
PDK
PKM
PDH
Acetyl-CoA
Pyruvate
LDH
Krebs cycle
Lactate

B

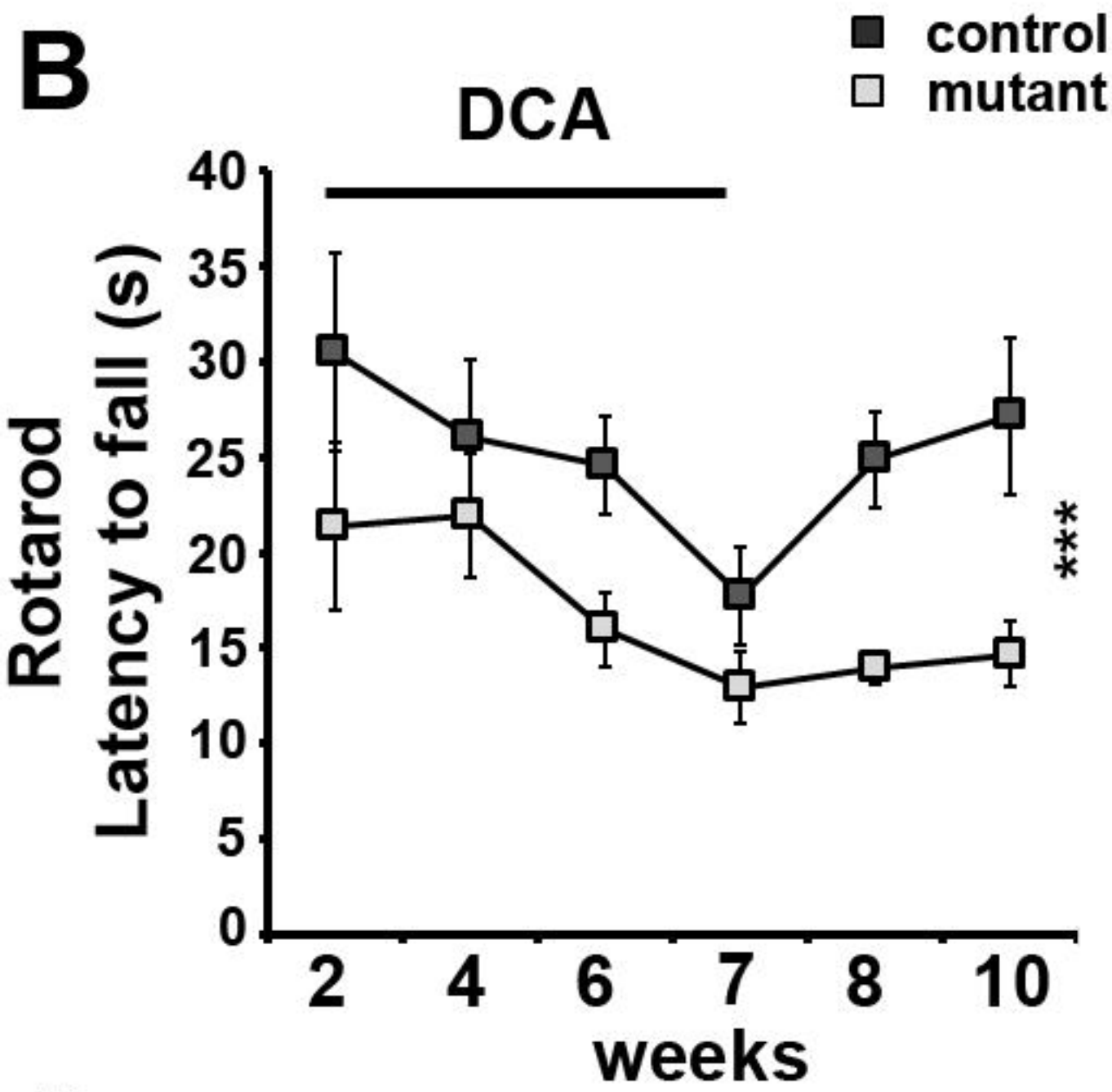
control
mutant
DCA
Rotarod
Latency to fall (s)
40
35
30
25
20
15
10
5
0
***
2
4
6
7
8
10
weeks

C

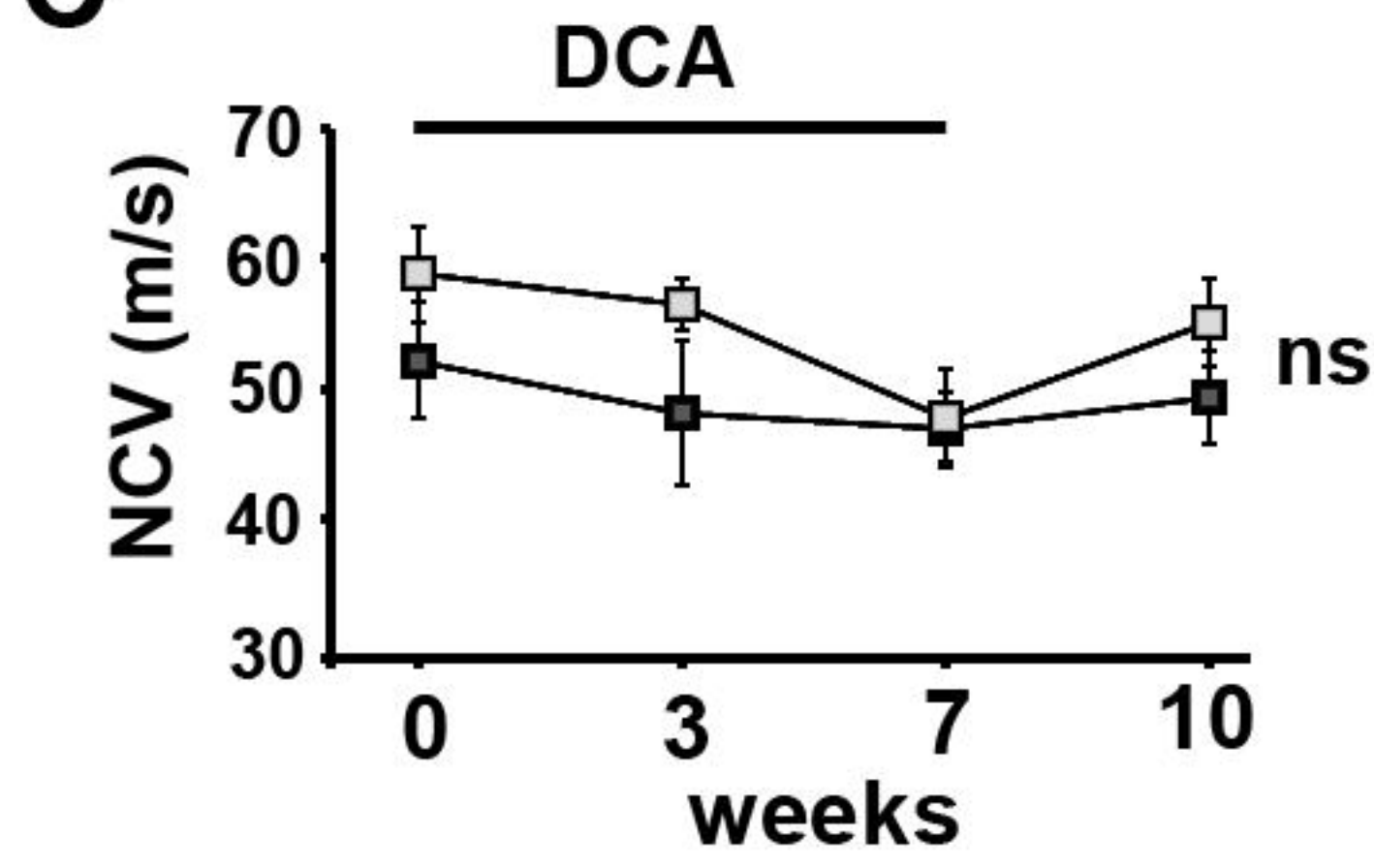
DCA
NCV (m/s)
70
60
50
40
30
ns
0
3
7
10
weeks